Journal of Food Engineering 109 (2012) 752–761

Contents lists available at SciVerse ScienceDirect

Journal of Food Engineering

journal homepage: www.elsevier.com/locate/jfoodeng

Study of optimization of the synthesis and properties of biocomposite films based on grafted chitosan

Adelaida Ávila [a], Karina Bierbrauer [b], Graciela Pucci [a], Mar López-González [c], Miriam Strumia [b,*]

[a] Facultad de Ciencias Naturales, Universidad Nacional de la Patagonia San Juan Bosco (U.N.P.S.J.B.), 9000 Comodoro Rivadavia, Argentina
[b] Facultad de Ciencias Químicas, Universidad Nacional de Córdoba (U.N.C.), IMBIV (Conicet), 5000 Córdoba, Argentina
[c] Instituto de Ciencia y Tecnología de Polímeros (CSIC), 28006 Madrid, Spain

ARTICLE INFO

Article history:
Received 6 August 2011
Received in revised form 5 November 2011
Accepted 7 November 2011
Available online 25 November 2011

Keywords:
Chitosan
HEMA
Grafted films
Food biodegradable covering

ABSTRACT

Acrylic acid (AcAc) and 2-hydroxyethyl methacrylate (HEMA) were graft copolymerized onto the chitosan backbone using radical initiation under different experimental conditions. The grafted products were then characterized by FTIR, TGA, grafting and swelling index (%*G* and *Q*, respectively), Mechanical properties and biodegradability were determined. The study of the properties of the grafted films demonstrated a marked influence of the concentration of acrylic monomers, time and temperature on the %*G*. In addition, both grafted films (CH-g-HEMA and CH-g-AcAc) showed a noticeable difference in their mechanical behavior. CH-g-HEMA stands the highest deformation for longer periods in relation to smaller strain values, whereas CH-g-AcAc shows better tension strain but lower deformation. Therefore, CH-g-HEMA films have a vast potential for food biodegradable covering characterized by their mechanical properties, non-toxicity and biodegradability.

1. Introduction

Chitosan is a natural cationic polymer with a structural polysaccharide commonly found in nature. Its unique chemical and biological properties have attracted attention because of the potential applications in areas, such as medicine, agriculture and industry. Undoubtedly, the main reasons for this involve its appealing intrinsic properties, such as biocompatibility, biodegradability, non-toxicity, film-forming ability, bioadhesivity, antimicrobial activity against fungi, bacteria and viruses.

Biodegradability and non-toxicity allow chitosan to be a promising material for drug delivery, packaging and biomedical devices (Andres et al., 2007; El Hadrami et al., 2010; Gupta and Haile, 2007; Harish Prashanth and Tharanathan, 2007; Sanpui et al., 2008; Zhang et al., 2010).

However, chitosan and other natural macromolecular materials such as agarose, dextran, cellulose and alginate, despite being good matrixes, are mechanically weak and often difficult to apply. Chemical modification of chitosan was sought to impart advantageous properties for synthesizing newer materials has increasingly drawn the attention of numerous studies; their main effort being centered on the introduction of a second component, a hydrophobic or hydrophilic polymer into the chitosan to form an IPN, a blend or grafted products (Bayramoglu et al., 2007; Chang et al., 2007; Chen et al., 2004; Rodkate et al., 2010; Vidyalakshmi et al., 2004; Wang et al., 2008) without a photosensitizer.

A variety of grafted copolymers of chitosan and vinyl monomers, including flocculants, ion-exchangers, drug delivery, affinity matrixes, were synthesized and evaluated (Casimiro et al., 2005; Dos Santos et al., 2006; Huang et al., 2006; Sánchez et al., 2007; Sashiwa and Aiba, 2004; Trong-Ming et al., 2006). This chemical combination of natural and synthetic polymers yields new materials, through which the beneficial properties of the natural polymer such as biodegradability and bioactivity remain unaltered. Graft copolymerization using methylmethacrylate, acrylonitrile, acrylamide, glycidylmethacrylate, acrylic acid or vinyl acetate has been reported utilizing a different kind of initiation such as Fenton's reagent, photo-induction with or without a photosensitizer or radical method under homogeneous and heterogeneous conditions (Bakhshi et al., 2009; Dergunov et al., 2008; Harish Prashanth and Tharanathan, 2003; Huang et al., 2007; Jalal Zohuriaan-Mehr, 2005; Liu et al., 2006; Lv et al., 2009; Zhou and Wu, 2011). In all cases interesting new properties were found, including thermal and physical stability, optimal swelling capacity, good barrier properties or improved mechanical properties.

HEMA (2-hydroxyethyl methacrylate) (Singh and Ray, 1998; Li et al., 2008) and acrylic acid (AcAc) (Jayakumar et al., 2011) are well known hydrogel-forming monomers widely applied in the graft copolymerization of chitosan to improve some properties or

* Corresponding author at: Departamento de Química Orgánica, Facultad de Ciencias Químicas, Universidad Nacional de Córdoba (UNC), 5000 Córdoba, Argentina. Tel./fax: +54 351 4333030.
E-mail address: mcs@fcq.unc.edu.ar (M. Strumia).

0260-8774/$ - see front matter © 2011 Elsevier Ltd. All rights reserved.
doi:10.1016/j.jfoodeng.2011.11.009

yield newer ones. Usually, they form three-dimensional-network hydrogels which could retain large quantities of water without dissolution. They exhibit high mechanical strength and resistance to many chemicals (Bayramoglu et al., 2007). Poly(acrylic acid) is widely used in adhesives and super absorbent materials since its pendant carboxylic groups are biocompatible and have antibacterial properties (Che et al., 2008; Güçlü et al., 2009).

On the other hand, it is well known that fruit and vegetables are perishable food, thus they need to be protected with some kind of film so as to prevent them from decaying. This protection blocks bacteria and other physical and chemical agents. Such covers must be innocuous, i.e., they should not in any way contaminate the food.

Nowadays, food packaging is usually made of PP, PE or PVC. These materials are non-biodegradable and expensive to recycle, constituting one of the main causes of environmental pollution. Therefore, biocomposite films pose an interesting research challenge in solving the future of packaging technology.

Although several studies on grafted chitosan have been reported, also using HEMA and AcAc, very few analyzed integrally their properties for their potential application as active packaging. The main objective of this research was to obtain biocomposite films with dual effects, i.e., good mechanical properties maintaining the advantageous properties of chitosan. These properties could give them interesting application as active and biodegradable food packaging material. With this purpose, AcAc and HEMA were graft-copolymerized onto the chitosan backbone using radical initiation under different experimental conditions without using any toxic crosslinkers. The grafted products were then characterized by FTIR and TGA. The swelling degree, mechanical properties and biodegradability of the films were evaluated.

2. Materials and methods

2.1. Materials

The materials and reactives used were: low molecular weight chitosan (CH, Aldrich) with a 15.5 acetylation degree, 345 KDa Mw; acetic acid solution HOAc 0.33 M (2% w/v); phosphate buffer (pH = 7.4); 2-hydroxyethyl methacrylate (HEMA, Sigma); acrylic acid (AcAc, Fluka); ethanol (Merck); ammonium persulfate (APS, Anedra). All reagents were of analytical grade and used without purification.

2.2. Equipment

ATR spectra were carried out on a FTIR Perkin-Elmer 520 Spectrum One spectrometer. The data were collected using 4 scans, nominal incident angle 45°. An internal reflexion diamond crystal was used. The same pressure was applied on each sample over crystal area.

Thermogravimetric measurements (TGA) of the polymers were carried out on a Perkin–Elmer TGA-7 precision thermogravimetric analyzer, in a nitrogen atmosphere, in the temperature range of 40–600 °C and at 10 °C/min heating rate.

2.3. Graft copolymerization reactions

The general procedure carried out for these reactions was: 45 mL of 2% w/v of low molecular weight chitosan (CH) stock solutions in acetic acid aqueous solution (HOAc, 0.33 M) were put in a flat-bottomed three-necked flask. Throughout the reaction time, nitrogen was purged at room temperature through the stirred solution. Freshly prepared potassium persulfate aqueous solution (2 mL, 7.4 mM) was added followed by dropwise addition of an aqueous solution 0.11 M of HEMA or AcAc. The reaction was conducted for different periods of time ranging from 2 to 4 h with stirring at different temperatures (35, 50, 65, and 73 °C). Table 1 displays the reaction conditions and quantities used to prepare the grafted samples. The reaction product was then precipitated out with 5% ammonium hydroxide (NH_4OH) solution until obtaining a uniform gel. The precipitate was filtered and washed with distilled water to remove the excess alkali; it was then exhaustively washed with ethanol for the complete removal of homopolymer. To insure that no residual monomers were left in the products, the final extraction solvent was analyzed by UV spectroscopy. No signal was obtained, showing that all the monomers were already extracted. The grafted copolymers (CH-g-HEMA and CH-g-AcAc) were dried in a vacuum desiccator.

The grafted percentage (%G) with respect to chitosan was gravimetrically analyzed in according to the variables studied: monomer concentration, reaction time, pH and temperature in CH-g-HEMA and CH-g-AcAc films, as seen in Eq. (1):

$$\%G = \left[\frac{\text{weight of grafted copolymer} - \text{weight of chitosan}}{\text{weight of chitosan}}\right] \times 100 \quad (1)$$

2.4. Preparation of the films

A known weight of pure and grafted chitosan (previously washed and purified as was indicated in 2.3) was dissolved in 2% w/v acetic acid solution to obtain 1% w/v solution, which was then stirred for 50 min and filtered to remove any non dissolved impurities. Thirty milliliter of the solutions were then poured on glass plate and dried at room temperature for 24 h and then at 30 °C for others 24 h in an oven. After cooling, the films were peeled off from the plate, and stored at room temperature (20 °C, 30% HR) until used.

2.5. Swelling index (Q)

Dried samples (Wd) were immersed in distilled water for 24 h. The swollen samples (Ws) were removed from the solution, quickly wiped with filter paper and weighed. The maximum water uptake (Q) of films was determined according to the following expression of Eq. (2):

$$Q = \left[\frac{\text{Ws} - \text{Wd}}{\text{Wd}}\right] \times 100 \quad (2)$$

2.6. Mechanical properties

Tensile tests were measured with an Instron Universal dynamometer at room temperature equipped with a 0.1 kN load cell. The membrane thickness ranged from 80 to 110 μm. Tensile stress (TS) was expressed in MPa and calculated by dividing the maximum load (N) by the initial cross-sectional area (m^2) of the specimen.

Table 1
CH (g), HEMA (mL) and AcAc (mL) used to prepared CH-g-HEMA and CH-g-AcAc.

CH:acrylic monomer (molar ratio)	CH (g)	HEMA (mL)	AcAc (mL)
1:0.5	0.9003	0.35	0.18
1:1	0.9002	0.68	0.37
1:3	0.9007	2.04	1.15
1:6	0.9005	4.08	2.25

Strain (ε) was calculated as the ratio of the final length at the point of sample rupture to the initial length of a specimen (20 mm) and expressed as a percentage. For each polymer sample at least five test tubes were used.

2.7. Permeability studies

2.7.1. Oxygen permeation measurements

High vacuum was made in an experimental permeation device made up of two compartments separated by the film. One of the compartments, the upstream chamber, was filled with oxygen, carbon dioxide or hydrogen gases at a given pressure and the permeation of the gas through the film to the other compartment, or downstream chamber, was monitored as a function of time with a MKS pressure sensor (10^{-4}–1 mmHg) via a PC. The permeation equipment was immersed in a water thermostat at the temperature of interest 30 °C.

The permeation coefficient, P, was obtained by means of the following expression:

$$P = \frac{273}{76}\left[\frac{V_d L}{A T p_u}\right]\lim_{t\to\infty}\frac{dp_d(t)}{dt} \tag{3}$$

where V_d, A, L, and T represent, respectively, the volume of the downstream chamber, the barrier of the permeation area, the membrane thickness and temperature. The variables p_d and p_u are the pressures of the downstream and upstream chambers, respectively. Usually, the permeability coefficient is given in barrers [1 barrer = $10^{-10}\times$ cm^3(STP)/(cm^2 s cmHg)].

2.7.2. Water vapor permeability measurements (WVP)

WVP was determined in duplicate for all films according to the desiccant method described in the ASTM standard method (ASTM E96M-10, 2010). Each film of 38.5 cm^2 was sealed onto an aluminum permeation cup (50 mm in diameter and 17 mm in depth) containing dry $CaCl_2$ (0% RH) with silicone vacuum grease and a ring to hold the film in place. The side in contact with the casting plate surface was exposed inside the test cups. Once the films were held, the test cells were then placed in a humidity chamber at (70 ± 2) %RH and 25 °C. The permeability cups with the films were weighted at intervals of 1 h during 12 h. Linear regression was used to calculate the slope of a fitted straight line in a graph of variation of mass versus time. The water vapor transmission rate (WVTR) (kg s^{-1} m^{-2}) and the WVP (kg m Pa^{-1} s^{-1} m^{-2}) were calculated from Eqs. (4) and (5), respectively:

$$\mathrm{WVTR} = F/A \tag{4}$$

$$\mathrm{WVP} = (\mathrm{WVTR}\times e)/[S_p\times(RH_1 - RH_2)] \tag{5}$$

where F is the slope of the graph of variation of mass versus time (kg s^{-1}), A is the test area (cup mouth area), e is the film thickness (m), S_p is the saturation pressure (Pa) at the test temperature, RH_1 is the relative humidity in the humidity chamber, and RH_2 is the relative humidity inside the cell test.

2.8. Biodegradation process

The biodegradability test by composting on a laboratory-scale was performed on the basis of ISO 14855 (1999): "Determination of the ultimate aerobic biodegradability and disintegration of plastic under controlled composting conditions". The tests were conducted in aerobic compost reactors at 25 °C, 60% moisture, and using municipal waste mixture. The studies were carried out using three replicate test reactors, three replicate samples in each test reactor for each exposure time. Two blank reactors were included in this biodegradation testing system. The blank reactors contained only 90 g of municipal waste mixture. In the reference or test reactors, CH film was mixed with municipal soil. The biodegradability of CH and CH-g-HEMA films was determined by measuring the amount of CO_2 trapped every 2 days and relating the results to the calculated percent of the theoretical CO_2 production (Eq. (6)), on the basis of the theoretical weight of the material under investigation. The experiments were done on two different types of municipal waste: pristine municipal waste was first used; the assays were then made on the waste used previously and already enriched with the degradation bacteria of the biocomposite films studied:

$$\mathrm{Quitosan} + O_2 \rightarrow \mathrm{Biomass} + CO_2 + H_2O \tag{6}$$

In principle, the carbon dioxide released from the system of production is fixed in sodium hydroxide and carbonate formed is titrated with hydrochloric acid.

The reaction of CO_2 production was followed by a two-step reaction (Kale et al., 2007). To determine the amount of CO_2 produced, the alkaline solution was titrated with 0.085 N HCl with two end points followed by two indicators: phenolphthalein and heliantina.

The amount of CO_2 produced by the biodegradation was calculated using the following Equation:

$$m_{CO2}(g) = 2\times V_2\times C_{HCl}\times\frac{44}{2.000}\times\frac{2.0\,\mathrm{mL}}{0.5\,\mathrm{mL}} \tag{7}$$

In which V_2 is the volume of spent acid in the titration using heliantina as indicator, C_{HCl} is the concentration of standard solution of HCl and 44 is the molar mass of CO_2.

The % Biodegradation was calculated according to Eq. (8):

$$\%\ \mathrm{Biodegradation} = \frac{(CO_2)_T - (CO_2)_B}{(CO_2)_{teor}}\times 100 \tag{8}$$

where $(CO_2)_T$ (g) is the cumulative amount of CO_2 released per sample, $(CO_2)_B$ (g) is the cumulative amount of CO_2 by the blank experiment and $(CO_2)_{teor}$ (g) is the theoretical amount of CO_2 produced by the film.

3. Results and discussion

3.1. Synthesis

Polymer grafting reactions provide the potential for significantly altering the physical and mechanical properties of the starting materials. Some grafted polymers tend to form thin films, which may be useful for packaging applications. Polymer grafting is usually carried out by radical initiation, which is done either by photoinduced free radical or free radicals initiators. For the former, the main disadvantage lies in the formation of homopolymers, because the UV light generates free radicals directly on vinyl monomers, thereby increasing homopolymerization (Harish Prashanth and Tharanathan, 2003), whereas with radical initiators the free radicals are produced on specific sites, also increasing the grafting efficiency. The reactive C-2 amino groups in chitosan readily react in free radical initiated copolymerization. Therefore, they are involved in the macroradical formation. However, we propose the formation of grafted polyHEMA or polyAcAc onto chitosan chains took place through the NH_2 group with partial formation of an interpenetrating network and also crosslinkage between the different chains. In the present research, ammonium persulfate was used in different concentrations as a free radical initiator to induce grafting. HEMA and AcAc were chosen as monomers to graft the chitosan at different initial concentrations, and at variable reaction times and temperatures. Fig. 1 shows the scheme of formation of the different types of networks.

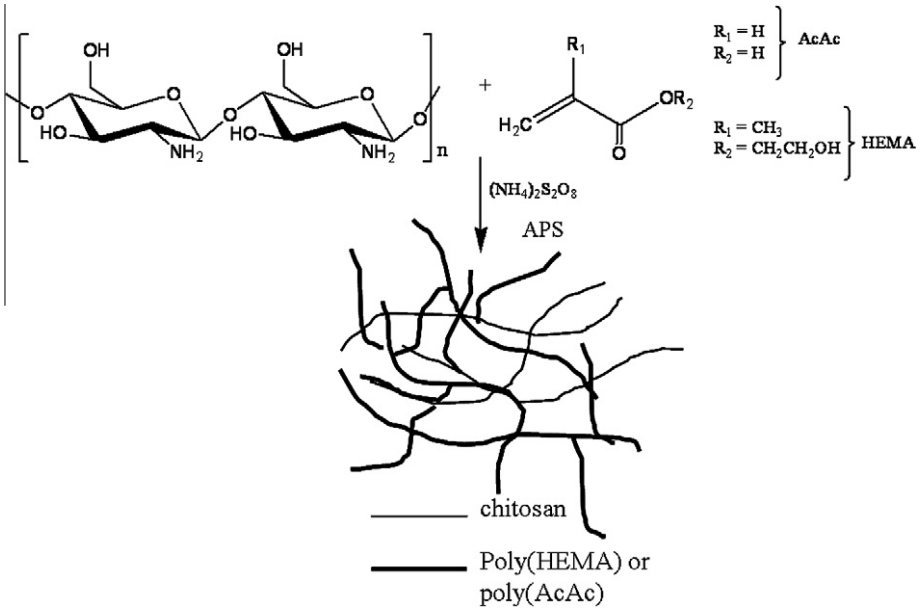

Fig. 1. Scheme of grafted chitosan using acrylic acid or HEMA as monomers.

Table 2
Molar composition, grafting percentage and swelling index of CH-g-HEMA and CH-g-AcAc at 65 °C and 3 h reaction time.

CH:HEMA (molar ratio)	Grafting (%)	Swelling index	CH:AcAc (molar ratio)	Grafting (%)	Swelling index
Chitosan	0.0	11.9	Chitosan	0.0	11.9
1:0.5	10.1	5.1	1:0.3	9.8	20.1
1:1	23.5	18.4	1:1	15.0	24.5
1:3	91.2	8.9	1:3	32.8	14.4
1:6	165.7	5.9	1:6	82.3	6.3

3.1.1. Effect of monomer concentration

Table 2 shows the results of the grafted reaction of chitosan with varying amounts of HEMA or AcAc. As seen, in both cases, an increase in the grafting percentage correlates with an increase in monomer concentration. However, the grafting reactions were more effective using HEMA monomers than those of AcAc.

Probably, the reactivity of HEMA to copolymerize with CH is better than that of AcAc, which could be more likely to homopolymerize.

3.1.2. Effect of reaction temperature

Fig. 2 shows the graft content for the grafting reactions with HEMA and AcAc onto chitosan using a ratio of 1:1 and pH 4.5 at different temperatures. In the grafted films of CH-g-HEMA, the graft content initially increases with temperature at 35 °C, and then slowly decreases. However, the influence of the temperature on the grafted reactions does not have a pronounced effect (range of 10–15%). In CH-g-AcAc samples, the best graft content was observed at 65 °C, due to the enhanced diffusion of monomer molecules to the macroradical sites. Further to an increase in the temperature results in a decrease in the graft content. This is expected when the chain transfer reactions with higher activation energy could be favored at higher temperatures and in many cases, this contributes more to an homopolymerization instead to a grafting reaction. Besides, higher temperatures could contribute to a degradation process of CH.

3.1.3. Effect of reaction time

Fig. 3 shows the variation of grafting reactions with time on samples prepared using a ratio of 1:1, temperature 65 °C and pH 4.5. It is observed that the time for obtaining the higher grafting

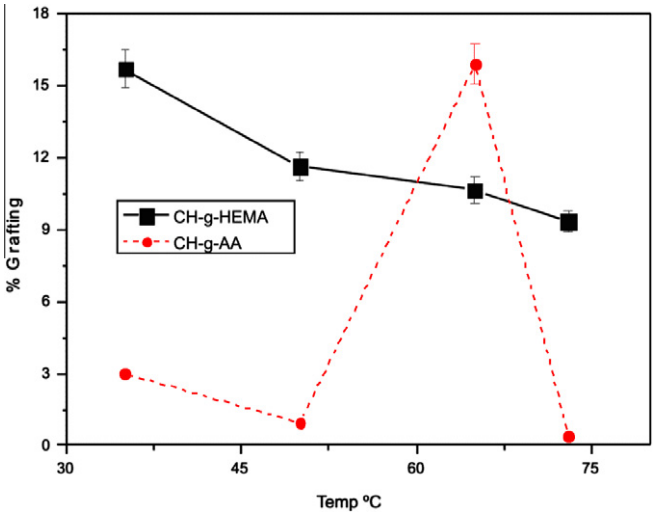

Fig. 2. Effect of temperature on the %*G* of CH-g-HEMA and CH-g-AcAc.

reaction degree was two hours on CH-g-HEMA and three hours on CH-g-AcAc. These results confirm that the effectiveness of the grafting on chitosan is higher with HEMA than with AcAc.

3.2. Characterization

3.2.1. Spectroscopy characterization

The changes in the structure of grafted chitosan (CH-g-HEMA and CH-g-AcAc) were examined by ATR FTIR spectroscopy as

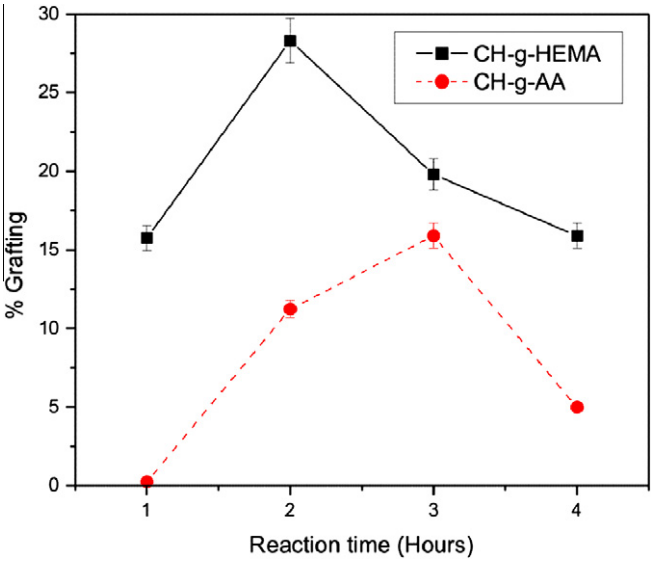

Fig. 3. Effect of reaction time on %*G* of CH-g-HEMA and CH-g-AcAc.

shown in Figs. 4 and 5, respectively. The IR spectra (Fig. 4) show characteristic absorption bands of chitosan at 3350–3200 cm^{-1} (O–H and N–H), 1656 cm^{-1} (amide I), 1528 cm^{-1} ($-NH_2$ bending) and 1381 cm^{-1} ($-CH_2-$ bending). The absorption bands at 1156 (anti-symmetric stretching of the C–O–C bridge), 1084 and 1028 cm^{-1} (skeletal vibrations involving the C–O stretching) are characteristic of saccharide structure. As seen in the final products, the band (–C=O, ester) of poly(HEMA) chains appears at 1728 cm^{-1}, demonstrating the presence of these polymers in the grafted chitosan networks. The band (–C=C–, conjugated with the carbonyl group) characteristic of monomer HEMA at 1640 cm^{-1} disappears as a result of the copolymerization.

The ATR spectra of the CH-g-AcAc are shown in Fig. 5. Previous studies report that the absorption peak of carboxyl groups in pure poly(acrylic acid) appears at 1720 cm^{-1} (Liu et al., 2008a,b). Two new absorption bands at 1720 cm^{-1} and 1545 cm^{-1}can be assigned to the absorption peaks of the carbonyl groups and carboxylate anion of poly(AcAc) covalently bonded onto chitosan chain. These results indicate that the carboxylic groups of poly(AcAc) chain are dissociated into COO^- groups(reaction pH was 4.5) which attract protonated amino groups of CH through electrostatic interaction to form complex polyelectrolyte during the polymerization procedure.

3.2.2. Swelling

The swelling indexes (*Q*) of the CH-g-HEMA and CH-g-AcAc products in water were previously shown in Table 2.

Chitosan films grafted with AcAc were able to absorb higher contents of water than HEMA grafted chains. It is known that polyelectrolyte salt formation produces an increase in swelling in aqueous solution. In the range explored, the chitosan:acrylic monomer (1:1) relationship showed the highest swelling indexes. This behavior could be assigned to the fact that these grafted chains have the optimal length to give steric hindrance to the hydrogen bond formation, characteristic of the native chitosan chain.

The films with lower and higher grafting percentages showed lower swelling indexes in both cases. This could be explained as follows: for those samples in which there is a higher composition of one of the components, the other one could act as an intercrossing agent through secondary forces (hydrogen bond or electrostatic interactions), resulting in a net collapse. In addition, the probable crosslinking of HEMA and AcAc chains in the polymer network at the highest grafting ratio may be responsible for the decrease in swelling of grafted samples. The hydrophilic nature of chitosan results from the presence of free amino groups on the C-2 carbon.

During the grafting process, a substantial number of free amino groups are blocked by the growing chains of the HEMA and AcAc. These changes are also responsible for the decrease in swelling.

3.2.3. Thermogravimetric analysis

Fig. 6a and b shows the corresponding thermogravimetric curves (weight loss % in relation to temperature) and their first derivative curves of chitosan, CH-g-HEMA and CH-g-AcAc, respectively.

The TGA of pure chitosan shows a weight loss in two stages. The first stage ranges between 40 °C and 200 °C with about 15% weight loss. This may be attributed to the adsorbed and bound water. The

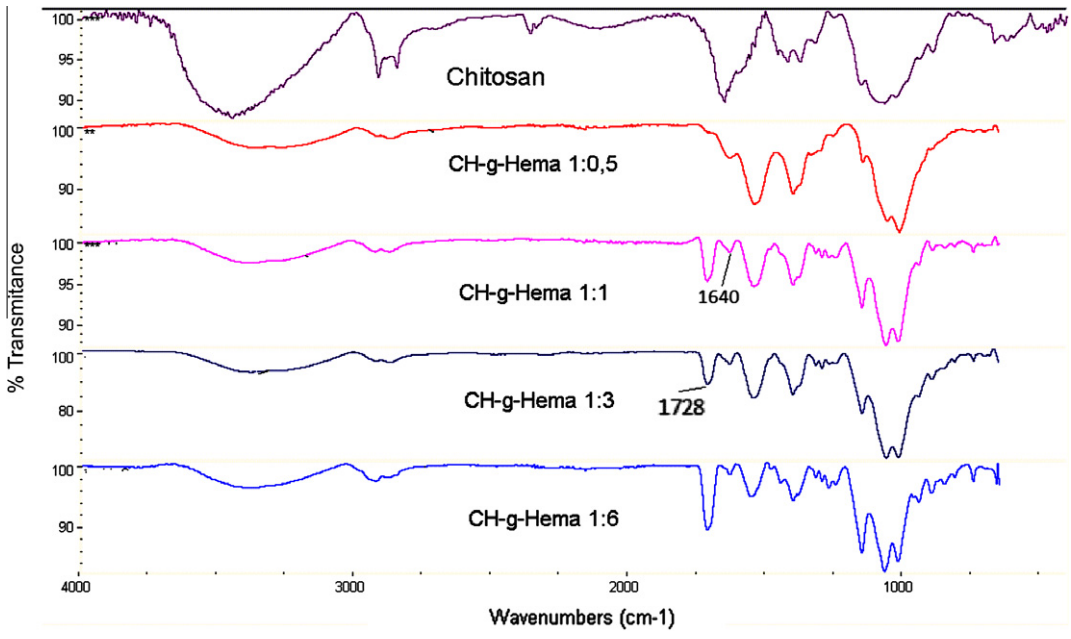

Fig. 4. FTIR-ATR spectra of chitosan and CH-g-HEMA films at different molar ratios: 1:0.5; 1:1; 1:3; 1:6.

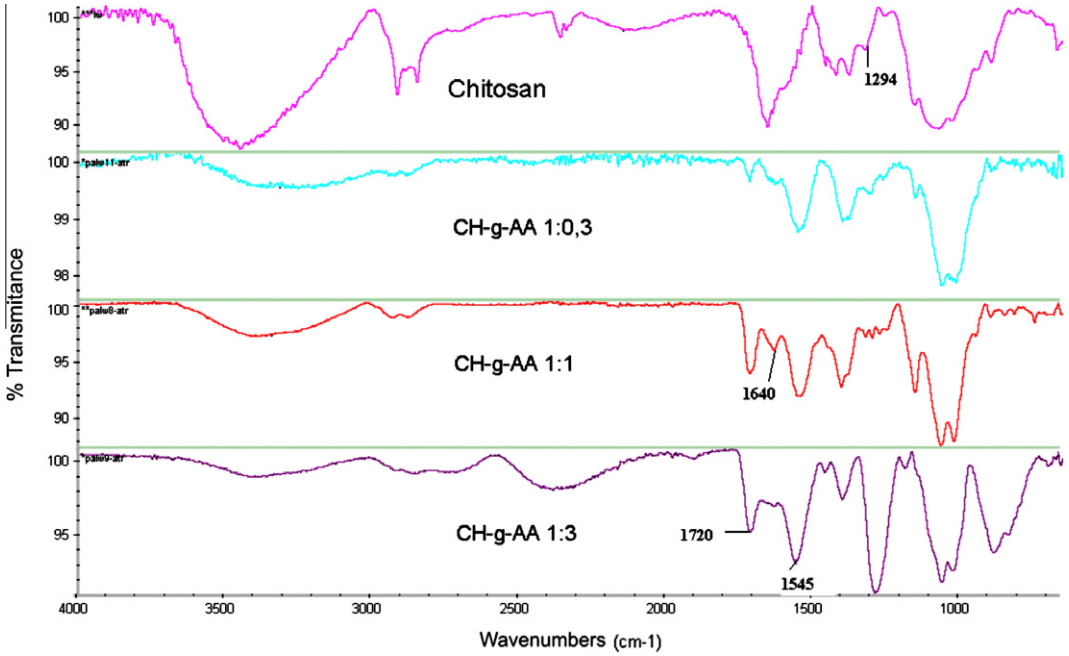

Fig. 5. FTIR-ATR spectra of chitosan and CH-g-AcAc films at different molar ratios: 1:0.3; 1:1; 1:3.

second stage of weight loss starts at 200 °C and continues up to 300 °C. There was about 40% of weight loss due to the degradation of polysaccharide. The TGA and its first derivative curve of CH-g-HEMA sample (Figs. 6a and 7a respectively) undergo weight loss in two stages at a lower grafting degree and in three stages at a higher grafting degree. During the first stage, which starts from 40 °C and continues up to 200 °C, there is about 15% weight loss of adsorbed and bound water in all the films. In the second stage, which ranges between 200 °C and 350 °C in the CH-g-HEMA 1:0.5 and 1:1 samples, there is a weight loss of about 30%. This may be due to the degradation of grafted chains in the films. When the molar ratios used are 1:3 and 1:6, a third stage appears up to 450 °C (Kashiwazaki et al., 2009). This coincides with the presence of another maximum as shown in Table 3, due to the degradation of chitosan backbone by random chain scission.

The same behavior was observed for CH-g-AcAc (Figs. 6b and 7b). The first stage ranges between 40 °C and 200 °C with a molar ratio of 1:3 and 250 °C in the molar ratio of 1:1 and 1:0.3. The graphic also shows about a 10% weight loss in the film with a molar ratio of 1:3 and 25% weight loss in the molar ratio of 1:0.3 and 1:1. This may be due to the loss of adsorbed water. In the second stage, which ranges between 200 °C and 400 °C in 1:3 sample, there is about 30% weight loss due to the degradation of the external chains of the grafted chitosan (Kashiwazaki et al., 2009). A third stage appears up to 385 °C in CH-g-AcAc 1:1 and 1:3, due to the degradation of synthetic polymer.

The TGA data clearly indicate that the stability of chitosan has been decreased by grafting with hydrophilic HEMA and AcAc. When the unmodified chitosan is compared with the derivatives of the grafted chitosan, we observe lower thermal degradation temperatures and more degradation steps, especially when *%G* increases.

3.2.4. Mechanical properties

Mechanical properties of chitosan, CH-g-HEMA and CH-g-AcAc films of tensile stress are found in Figs. 8 and 9. They show the effect of different concentrations of monomer agents incorporated into films and the consequent change in the properties. In the

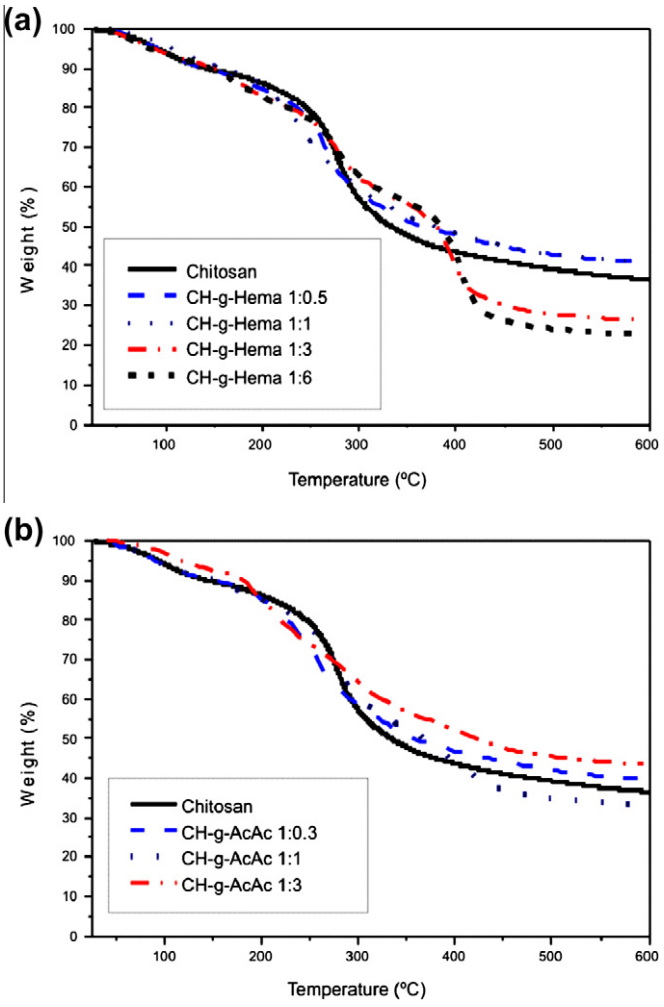

Fig. 6. Thermogravimetric analysis curves of CH, CH-g-HEMA (a) and CH-g-AcAc (b) films.

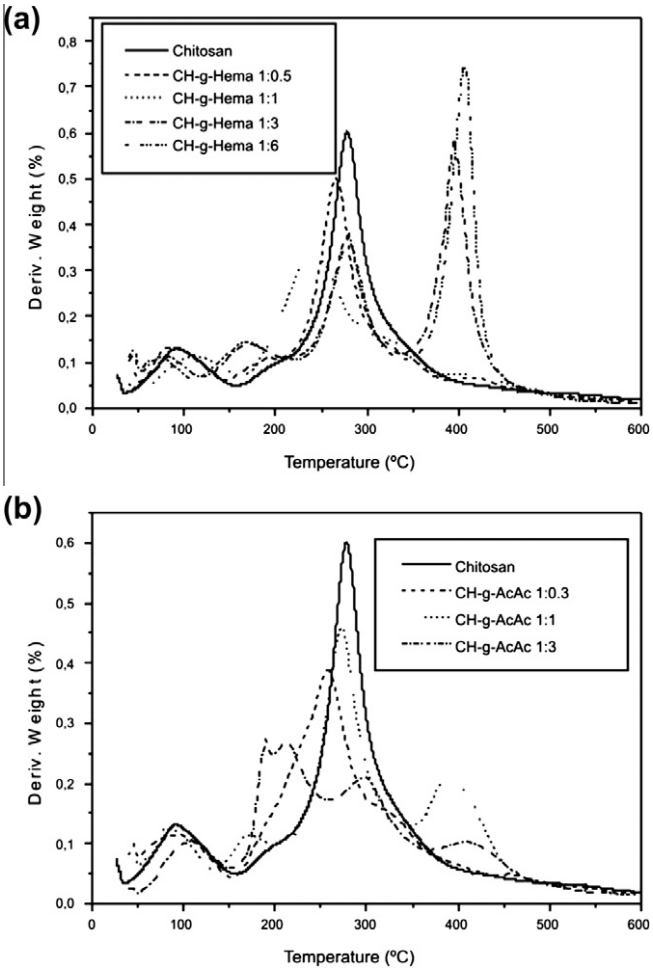

Fig. 7. First derivative curves of CH, CH-g-HEMA (a) and CH-g-AcAc (b) films.

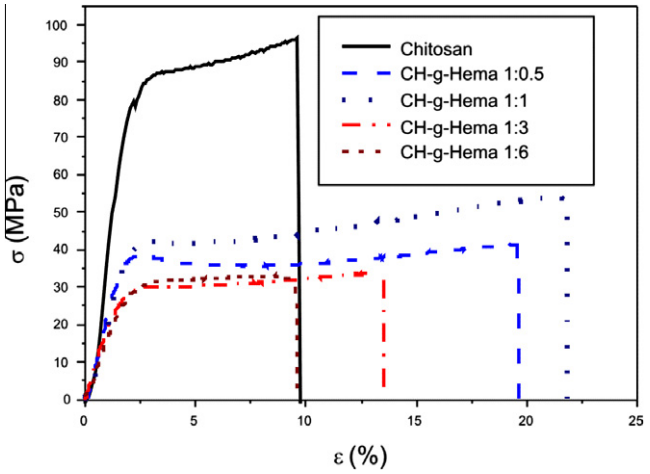

Fig. 8. Graphic representation of the stress (σ) in CH and CH-g-HEMA films in relation to deformation ε (%).

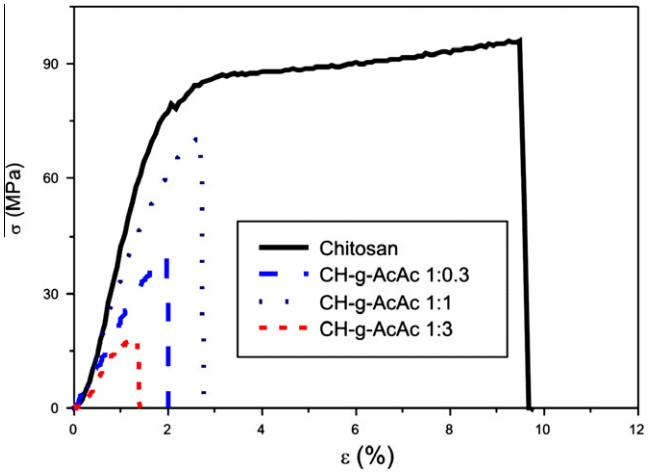

Fig. 9. Graphic representation of the stress (σ) in CH and CH-g-AcAc films in relation to deformation ε (%).

Table 3
Peak temperatures in TG during thermal degradation of chitosan, CH-g-HEMA and CH-g-AcAc films.

Sample	G (%)	IDT (°C)[a]	FDT (°C)[a]
Chitosan	0.0	248.2	349.2
CH-g-HEMA 1:0.5	10.1	249.3	334.5
CH-g-HEMA 1:1	23.5	218.9	356.8
CH-g-HEMA 1:3	91.2	277.6	437.6
CH-g-HEMA 1:6	165.7	277.6	409.0
CH-g-AcAc 1:0.3	9.8	241.0	361
CH-g-AcAc 1:1	15.0	218.0	372
CH-g-AcAc 1:3	32.8	213.2	372

[a] IDT: initial decomposition temperature, FDT: final decomposition temperature.

range of the deformation studied, a greater decrease in tensile stress is shown by the addition of HEMA and AcAc. The time and deformation supported by the films under stress have been evaluated.

Fig. 8 depicts the variation in stress in relation to the percentage of deformation in CH-g-HEMA for different molar relations. It has been observed that the 1:1 film undergoes the greatest stress values with longer periods of deformation rates up to 20%. The addition of high HEMA concentration lowered the deformation modulus of the film (Xu et al., 2005). This suggests that these films present a more thermoplastic behavior than that of chitosan without grafting.

CH-g-AcAc 1:1 membranes are observed to undergo small deformations under high stress values (Fig. 9). In CH-g-AcAc films the ε values always decreased when the ratio is increased. This shows that these films behave like fibers, i.e., that they can support high stress without deformation, but are fragile, brittle and easily broken. The tensile stress (TS) and deformation (ε) values at break of the CH-g-HEMA and CH-g-AcAc films with the different HEMA and AcAc ratios were obtained from Figs. 8 and 9, respectively and summarized in Table 4. These results indicate that the TS values of the films decrease first with the addition of synthetic polymer, then they reach maximum values at 71 MPa for CH-g-AcAc 1:1, and 54 MPa for CH-g-HEMA 1:1. The TS then decreases with a further increase in the grafting ratio. The decreasing TS values of the films, in the chitosan-monomer ratio of 0–0.5 and 1–6 could be attributable to the formation of intra-molecular hydrogen bonds of the synthetic polymer rather than to that of the inter-molecular hydrogen bonds, resulting in a phase separation between the two main components (Xu et al., 2005).

Young's moduli of the chitosan films were 4.7 GPa. The maximum value was observed at 3.3 GPa in CH-g-AcAc films 1:1 and 2.14 GPa in CH-g-HEMA films1:1. In the CH-g-HEMA films, the

Table 4
Tensile stress (TS) and deformation (ε) at break of chitosan, CH-g-HEMA and CH-g-AcAc films.

Sample	TS (MPa)	ε (%)
Chitosan	96	10
CH-g-HEMA 1:0.5	41	20
CH-g-HEMA 1:1	54	22
CH-g-HEMA 1:3	33	14
CH-g-HEMA 1:6	32	9
CH-g-AcAc 1:0.3	40	2
CH-g-AcAc 1:1	71	3
CH-g-AcAc 1:3	17	1

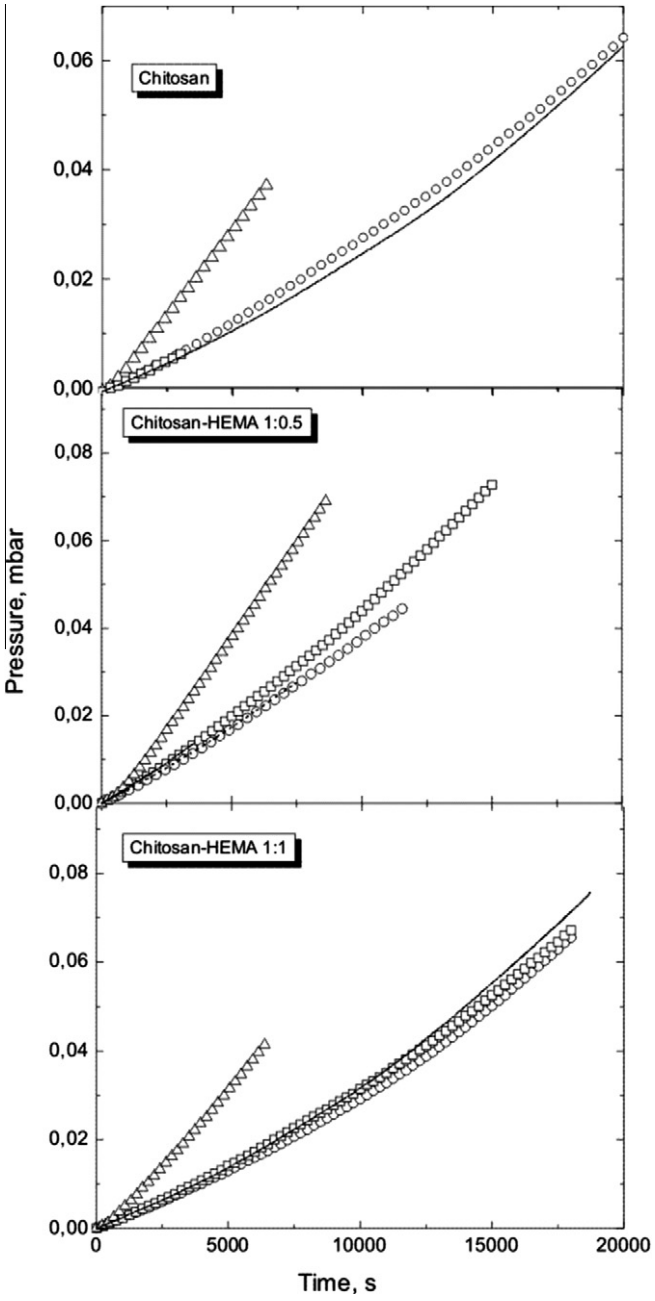

Fig. 10. Variation of the pressure of (□) oxygen, (○) carbon dioxide and (△) hydrogen as a function of time at 30 °C and 1 bar in chitosan (top), chitosan–HEMA 1:0.5 (middle) and Chitosan–HEMA 1:1 (bottom) membranes. Lines represent the leaks of the system.

Table 5
Water vapor permeability (WVP) values of CH and CH-g-HEMA films.

Films	WVP ($g/Pa^{-1}\ s^{-1}\ m^{-1}$)
CH	1.77×10^{-13}
CH-g-HEMA 1:0.5	2.00×10^{-13}
CH-g-HEMA 1:1	2.40×10^{-13}

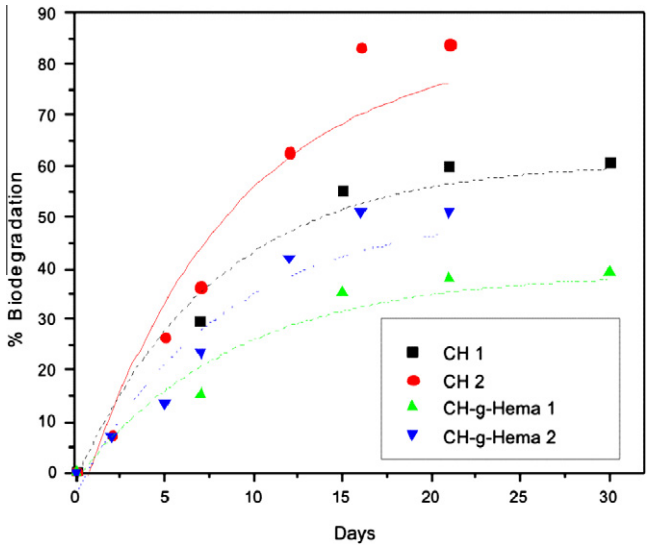

Fig. 11. Rate of biodegradation as a function of time in chitosan and CH-g-HEMA 1:1 films.

Young's moduli always decreased from the value obtained in the chitosan films. The CH-g-AcAc had a higher Young's modulus compared with that of CH-g-HEMA. This observation is most probably related to the reaction between amino groups of chitosan and carboxylic groups of AcAc from adjacent chains, resulting in the formation of a stiffer material.

Additionally, the T_g of poly(HEMA) is about 80 °C, differing from poly(AcAc) with a T_g of 106 °C. Dong et al. (2004) have reported that the T_g of chitosan is around 200 °C, which is very close to the degradation temperature onset. On the other hand, Dos Santos et al. (2006) have demonstrated through DMTA studies that grafted chitosan with HEMA shows a perfect miscibility between the poly(HEMA) and chitosan. This observation justifies the mechanical properties found in these results and the thermoplastic behavior of CH-g-HEMA.

3.2.5. Permeability studies

It is known that polysaccharides and proteins films have effective barriers to gases (El-Azzami and Grulke, 2007). Specifically, chitosan has low permeability to oxygen and carbon dioxide, and its permeability is dependent on the water content (Li et al., 2008). Fig. 10 shows the gas permeability of chitosan, comparatively with CH-g-HEMA 1:0.5 and 1:1. The covalent introduction of the HEMA by grafting decreases the permeability of quitosan. Probably, this could be explained due to the increase of the tortuosity of the grafted films.

Table 5 shows the WVP for chitosan and grafted films. It was observed that the WVP slowly increases with grafting and with the initial concentration of the HEMA. However, these WVP values are the same or lower than those found in other films frequently used for packaging (López-González and Riande, 2006; Berins, 1991). However, it is known that although the permeability to

gases in dried films of polysaccharides is low, if the material spends long time in contact with wet food, it swells and allows for an increase of its permeability to gases.

3.2.6. Biodegradation studies

The CH-g-HEMA films were chosen for performing biodegradation assays due to their optimal mechanical properties and their potential packaging applications.

Fig. 11 shows the rate of biodegradation of chitosan and CH-g-HEMA 1:1 films in terms of days of exposure to degraded environments.

In Section 2.7 two kinds of experiment were explained. In Fig. 11 they were named as CH1and CH2 of chitosan films and CH-g-HEMA 1 and CH-g-HEMA 2 of chitosan:HEMA 1:1 films used in experiments 1 and 2, respectively.

Fig. 11 shows, in all cases, two stages of the biodegradation process of the films, which can be defined as the biodegradation phase (linear portion of the curve) and the plateau. The phase of the biodegradation curve of almost all films showed a high slope generally observed in the first 10 days of experience; the biodegradation process would then become slower and produce a plateau.

The CH2 sample was placed for testing biodegradation in municipal waste in the same bottle in which the experiment of biodegradation had been carried out with the CH1 sample. It can be assumed that the waste on which we placed the CH2 sample was enriched with bacteria that had degraded the CH1 sample. This could provide insights into the fact that the percentage of biodegradation for CH2 and CH-g-HEMA 2 samples was higher than that of sample 1. Moreover, in only 20 days the CH2 sample degraded 85% at a rate greater than that of the CH1 sample, while CH-g-HEMA 2 films showed 45% of biodegradation during the same time. Probably, the fact that biodegradation only affects CH chains leads to a weakening of the network integrity.

4. Conclusion

The studies and characterization of the physical chemical properties of the grafted films demonstrated the major influence attributed to the concentration of acrylic monomers, time and temperature on the %*G*. In addition, both grafted films (CH-g-HEMA and CH-g-AcAc) showed a pronounced difference in their mechanical behavior. CH-g-HEMA supports the highest deformation for longer periods in relation to smaller tension strain, whereas CH-g-AcAc showed better tension strain but lower deformation.

Therefore, the films of CH-g-HEMA have a great potential for food biodegradable covering showing non-toxicity and biodegradability. Those films keep the chitosan advantages, namely, good barrier properties to oxygen penetration and very good protection properties of specific foods.

References

Andres, Y., Giraud, L., Gerente, C., Le Cloirec, P., 2007. Antibacterial effects of chitosan powder: mechanisms of action. Environmental Technology 28 (12), 1357–1363.

Bakhshi, H., Zohuriaan-Mehr, M.J., Bouhendi, H., Kabiri, K., 2009. Spectral and chemical determination of copolymer composition of poly(butyl acrylate-co-glycidyl methacrylate) from emulsion polymerization. Polymer Testing 28 (7), 730–736.

Bayramoglu, G., Oktem, H., Arica, Y., 2007. A dye–ligand immobilized poly(2-hydroxyethylmethacrylate) membrane used for adsorption and isolation of immunoglobulin G. Biochemical Engineering Journal 34 (2), 147–155.

Berins, M., 1991. Plastics Engineering Handbook. Van Nostrand Reinhold, New York (pp. 102132).

Casimiro, M., Botelho, M., Leal, J., Gil, M., 2005. Study on chemical, UV and gamma radiation-induced grafting of HEMA onto chitosan. Radiation Physics and Chemistry 72, 731–735.

Chang, S., Niu, C., Huang, C., Kuo, S., 2007. Evaluation of chitosan-g-PEG copolymer for cell anti-adhesion application. Journal of Medical and Biological Engineering 27 (1), 41–46.

Che, A., Liu, Z., Huang, X., Wang, Z., Xu, Z., 2008. Chitosan-modified poly(acrylonitrile-co-acrylic acid) nanofibrous membranes for the immobilization of concanavalin A. Biomacromolecules 9 (12), 3397–3403.

Chen, Z., Deng, M., Chen, Y., He, G., Wu, M., Wang, J., 2004. Preparation and performance of cellulose acetate/polyethyleneimine blend microfiltration membranes and their applications. Journal of Membrane Science 235, 73–86.

Dergunov, S., Nam, I., Maimakov, T., Nurkeeva, Z., Shaikhutdinov, E., Mun, G., 2008. Study on radiation-induced grafting of hydrophilic monomers onto chitosan. Journal of Applied Polymer Science 110 (1), 558–563.

Dong, Y., Ruan, Y., Wang, H., Zhao, Y., Bi, D., 2004. Studies on glass transition temperature of chitosan with four techniques. Journal of Applied Polymer Science 93, 1553–1558.

Dos Santos, K.S., Coelho, J.F., Ferreira, P., Pinto, I., Lorenzetti, S., Ferreira, E., Higa, O., Gil, M., 2006. Synthesis and characterization of membranes obtained by graft copolymerization of 2-hydroxyethyl methacrylate and acrylic acid onto chitosan. International Journal of Pharmaceutics 310, 37–45.

El-Azzami, L.A., Grulke, E.A., 2007. Dual mode model for mixed gas permeation of CO_2, H_2, and N_2 through a dry chitosan membrane. Journal of Polymer Science Part B: Polymer Physics 45, 2620–2631.

El Hadrami, A., Adam, L., El Hadrami, I., Daayf, F., 2010. Chitosan in plant protection. Marine Drugs 8 (4), 968–987.

Güçlü, G., Al, E., Emik, S., İyim, T., Özgümüş, S., Özyürek, M., 2009. Removal of Cu^{2+} and Pb^{2+} ions from aqueous solutions by starch-graft-acrylic acid/montmorillonite superabsorbent nanocomposite hydrogels. Polymer Bulletin 65 (4), 333–346.

Gupta, D., Haile, A., 2007. Multifunctional properties of cotton fabric treated with chitosan and carboxymethyl chitosan. Carbohydrate Polymers 69 (1), 164–171.

Harish Prashanth, K.V., Tharanathan, R.N., 2003. Studies on graft copolymerization of chitosan with synthetic monomers. Carbohydrate Polymers 54, 343–351.

Harish Prashanth, K., Tharanathan, R., 2007. Chitin/chitosan: modifications and their unlimited application potential—an overview. Trends in Food Science and Technology 18 (3), 117–131.

Huang, M., Jin, X., Li, Y., Fang, Y., 2006. Syntheses and characterization of novel pH-sensitive graft copolymers of maleoylchitosan and poly(acrylic acid). Reactive and Functional Polymers 66 (10), 1041–1046.

Huang, Y., Yu, H., Xiao, C., 2007. pH-sensitive cationic guar gum/poly(acrylic acid) polyelectrolyte hydrogels: swelling and in vitro drug release. Carbohydrate Polymers 69 (4), 774–783.

Jalal Zohuriaan-Mehr, M., 2005. Advances in chitin and chitosan modification through graft copolymerization: a comprehensive review. Iranian Polymer Journal 14 (3), 235–265.

Jayakumar, R., Prabaharan, M., Sudheesh Kumar, P., Nair, S., Tamura, H., 2011. Biomaterials based on chitin and chitosan in wound dressing applications. Biotechnology Advances 29 (3), 322–337.

Kale, G., Auras, R., Singh, S.P., Narayan, R., 2007. Biodegradability of polylactide bottles in real and simulated composting conditions. Polymer Testing 26, 1049–1061.

Kashiwazaki, H., Kishiya, Y., Matsuda, A., Yamaguchi, K., Iizuka, T., Tanaka, J., Inoue, N., 2009. Fabrication of porous chitosan/hydroxyapatite nanocomposites: their mechanical and biological properties. Bio-Medical Materials and Engineering 19 (2–3), 133–140.

Li, X., Zhang, Y., Chen, G., 2008. Nanofibrous polyhydroxyalkanoate matrices as cell growth supporting materials. Biomaterials 29, 3720–3728.

Liu, Y., Zhang, R., Zhang, J., Zhou, W., Li, S., 2006. Graft copolymerization of sodium acrylate onto chitosan via redox polymerization. Iranian Polymer Journal 15 (12), 935–942.

Liu, L., Chakma, A., Feng, X., 2008a. Gas permeation through water-swollen hydrogel membranes. Journal of Membrane Science 310 (1–2), 66–75.

Liu, Z., Jiao, Y., Wang, Y., Zhou, C., Zhang, Z., 2008b. Polysaccharides-based nanoparticles as drug delivery systems. Advanced Drug Delivery Reviews 60, 1650–1662.

López-González, M., Riande, E., 2006. Criterios para conseguir materiales barrera a medida. Revista de Plásticos Modernos 91 (597), 241.

Lv, P., Bin, Y., Li, Y., Chen, R., Wang, X., Zhao, B., 2009. Studies on graft copolymerization of chitosan with acrylonitrile by the redox system. Polymer 50 (24), 5675–5680.

Rodkate, N., Wichai, U., Boontha, B., Rutnakornpituk, M., 2010. Semi-interpenetrating polymer network hydrogels between polydimethylsiloxane/polyethylene glycol and chitosan. Carbohydrate Polymers 81, 617–625.

Sánchez, A., Sibaja, M., Vega-Baudrit, J., Rojas, M., 2007. Utilización de soportes de hidrogel de quitosano obtenidos a partir de desechos del camarón langostino (pleuroncodes planipes) para el crecimiento in vitro de fibroblastos humanos. Revista Iberoamericana de Polímeros 8 (5), 347–362.

Sanpui, P., Murugadoss, A., Durga Prasad, P., Sankar Ghosh, S., Chattopadhya, A., 2008. The antibacterial properties of a novel chitosan-Ag-nanoparticle composite. International Journal of Food Microbiology 124 (2), 142–146.

Sashiwa, H., Aiba, S., 2004. Chemically modified chitin and chitosan as biomaterials. Progress in Polymer Science 29, 887–908.

Singh, D.K., Ray, A.R., 1998. Characterization of grafted chitosan films. Carbohydrate Polymers 36, 251–255.

Trong-Ming, D., Chia-Fong, K., Wen-Yen, C., Ching-An, P., 2006. Preparation and characterization of chitosan-g-poly(vinyl alcohol)/poly(vinyl alcohol) blends used for the evaluation of blood-contacting compatibility. Carbohydrate Polymers 63, 331–339.

Vidyalakshmi, K., Rashmi, K., Kumar, T., 2004. Studies on formation and in vitroevaluation of PVA/chitosan blend films for drug delivery. Journal of Macromolecular Science: Pure and Applied Chemistry 41, 1115–1122.
Wang, Q., Zhang, Na., Hu, X., Yang, J., Du, Y., 2008. Chitosan/polyethylene glycolblend fibers and their properties for drug controlled release. Journal of Biomedical Materials Research Part A 85 (4), 881–887.
Xu, Y.X., Kim, K.M., Hanna, M.A., Nag, D., 2005. Chitosan–starch composite film. Preparation and characterization. Industrial Crops and Products 21, 185–192.
Zhang, J., Xia, W., Liu, P., Cheng, Q., Tahirou, T., Gu, W., Li, Bo., 2010. Chitosan modification and pharmaceutical/biomedical applications. Marine Drugs 8, 1962–1987.
Zhou, C., Wu, Q., 2011. A novel polyacrylamide nanocomposite hydrogel reinforced with natural chitosan nanofibers. Colloids and Surfaces B: Biointerfaces 84 (1), 155–162.